Available online at www.sciencedirect.com

ScienceDirect

Procedia Materials Science 3 (2014) 1322 – 1329

Procedia Materials Science

www.elsevier.com/locate/procedia

20th European Conference on Fracture (ECF20)

Fracture mechanics analysis of heterogeneous welds: validation of a weld homogenisation approach

Stijn Hertelé[a,]*, Noel O'Dowd[b], Koen Van Minnebruggen[a], Matthias Verstraete[a], Wim De Waele[a]

[a]*Ghent University, Soete Laboratory, Technologiepark Zwijnaarde 903, 9052 Zwijnaarde, Belgium*
[b]*University of Limerick, Materials and Surface Science Institute, Limerick, Ireland*

Abstract

Flaw assessments assume homogeneous material properties, but welds are heterogeneous. The authors have developed a method to address heterogeneity in the estimation of crack driving force. This paper presents a numerical validation of the proposed approach. Weld heterogeneity is characterized in three pipeline girth welds by means of hardness mapping. The resulting distributions are input into a finite element model of a clamped SE(T) specimen. Following, crack tip opening displacement responses of heterogeneous welds are compared with predictions. The approach is found to strongly simplify analyses involving heterogeneous welds while maintaining an acceptable level of accuracy with respect to load.

Selection and peer-review under responsibility of the Norwegian University of Science and Technology (NTNU), Department of Structural Engineering

Keywords: girth weld, heterogeneity, hardness, SE(T), CTOD

1. Introduction

The integrity assessment of flawed structures requires a quantification of crack driving force under imposed loading conditions. Most flaw assessment procedures in elastic-plastic fracture mechanics assume a defect to be

* Corresponding author. Tel.: +32-(0)9-331-0474; fax: +32-(0)9-331-0490.
E-mail address: stijn.hertele@ugent.be

Selection and peer-review under responsibility of the Norwegian University of Science and Technology (NTNU), Department of Structural Engineering
doi:10.1016/j.mspro.2014.06.214

surrounded by homogeneous material (i.e. exhibiting a fixed constitutive behaviour). For instance, the EPRI framework for estimation of J by Kumar et al. (1981) assumes fixed true stress – true strain (σ-ε) properties, characterized by the well-known model of Ramberg and Osgood (1943):

$$\frac{\varepsilon}{\varepsilon_y} = \frac{\sigma}{\sigma_y} + \alpha\left(\frac{\sigma}{\sigma_y}\right)^n \tag{1}$$

Linear elasticity implies that σ_y/ε_y is Young's modulus E. It is challenging to assign unique values to the model parameters σ_y (yield strength), n (strain hardening exponent) and α (yield offset) in fusion welds, which are typically characterized by a wide variety of microstructures. For instance, yield strength variations up to 100 MPa have been observed in weld metal within a distance of 5 mm by Hertelé et al. (2013a). To date, there is no generic approach to account for such strongly variable strength distributions in a flaw assessment. Most research efforts in this direction – e.g. in the dedicated conference proceedings edited by Schwalbe and Koçak (1994, 1997) – have been confined to so-called 'idealised' welds, defined by straight fusion lines and homogeneous weld metal. Hereby, the strength of the weld metal is commonly represented by a yield strength mismatch $M = \sigma_{yw}/\sigma_{yb}$, subscripts 'w' and 'b' referring to weld and base metal, respectively.

Aiming to address the complex heterogeneous nature of fusion welds in flaw assessments, the authors have developed a framework to simplify ('homogenise') welds with continuously varying strength properties (Hertelé et al., 2013b). The crack is assumed to be located in the centre of a symmetrical weld. A major outcome is that complex heterogeneous welds may be represented by an equivalent idealised weld (Fig. 1), whose crack driving force can be determined using published relations as for instance reported in Kim and Schwalbe (2001). As regards strength properties, this idealised weld has an 'equivalent' yield strength mismatch M_{eq}, given by:

$$M_{eq} = \frac{\int_{\mathbf{OF}} M(s)\mathrm{d}s}{\|\mathbf{OF}\|} \tag{2}$$

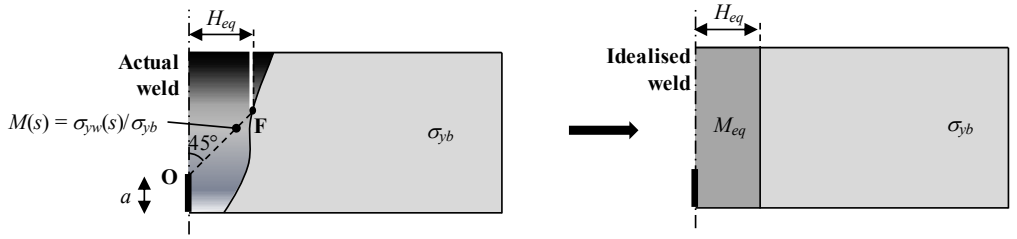

Fig. 1. Approach to derive an idealised weld from a complex weld, developed by Hertelé et al. (2013b).

with $M(s) = \sigma_{yw}(s)/\sigma_{yb}$, the local yield strength mismatch at a point on a path **OF**, describing the slip line trajectory originating from the crack tip (**O**) up to the weld fusion line (**F**). The cracked geometry is assumed to be loaded in tension, giving rise to theoretically straight slip lines at an angle of 45° to the surface (Hao et al., 1997; Kim, 2002). Equation (2) implies that average weld strength properties along **OF** govern the crack driving force. The half width of the idealised weld H_{eq} is equal to the horizontal projection of **OF**.

The homogenisation framework was validated using finite element analysis in Hertelé et al. (2013b). The clamped single-edge notched tension or $SE(T)_c$ test was taken as a research subject. Although successful, the validation was performed for a highly simplified case: (1) The finite element model was two-dimensional, assuming plane strain conditions; (2) A small-strain formulation was adopted. As a consequence, collapse phenomena (characterized by a drop in load) could not be modelled; (3) A simplified case of weld heterogeneity was assumed, namely V-shaped welds consisting of two areas (representing root and cap metal) with different, but fixed stress-

strain properties. Heat affected zone (HAZ) properties were not taken into account; (4) Heterogeneity was confined to yield strength variations, i.e. the strain hardening exponent was kept constant; (5) Cracks were located in the weld metal centre as also assumed for the development of the framework (Fig. 1).

Recognizing the severity of these simplifications, this paper evaluates the homogenisation approach in a new numerical study considering more realistic cases of weld heterogeneity. The paper is structured as follows. Section 2 presents the details of the validation approach. Attention goes to an experimental characterization of complex (i.e., heterogeneous) welds, the adopted finite element model, and the performed parametric study. Results are provided and discussed in section 3 and conclusions are drawn in section 4.

2. Validation study

2.1. Heterogeneous welds

Three steel pipeline girth welds were evaluated by means of Vickers hardness (HV) mapping. One weld (‘G’) was produced by gas metal arc welding, two others (‘S1’ and ‘S2’) by shielded metal arc welding. Polished and etched macro sections of each weld were indented with a load of 5 kg (‘HV5’) at roughly four positions per mm². This enabled the creation of hardness contour maps covering weld metal and adjacent HAZs and base metals, Fig. 2. The welds were chosen for this study because of their significant weld metal heterogeneity. Traversing from weld root to weld cap as indicated by dashed lines in Fig. 2, Vickers hardness varies within a significant range relative to the average base metal hardness: 21% (‘G’), 36% (‘S1’) and 24% (‘S2’). For welds ‘G’ and ‘S1’, hardness gradients mostly occur in the through-thickness direction. Weld ‘S2’ is more complex as peak hardness values occur in a V-shaped area of grain refined metal. Weld ‘G’ has softened HAZs as opposed to welds ‘S1’ and ‘S2’.

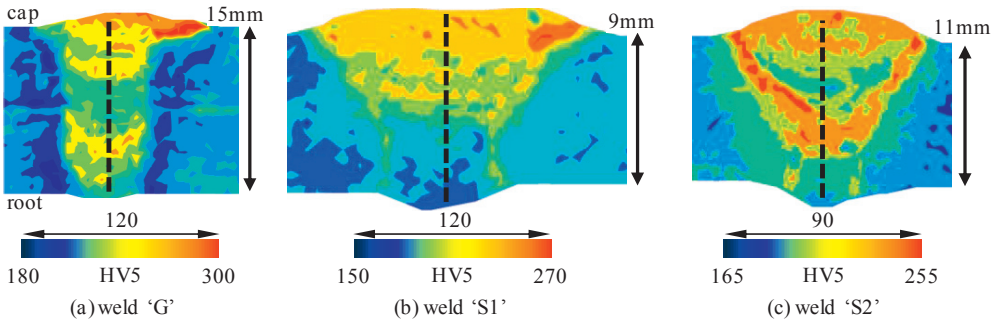

Fig. 2. Hardness (HV5) contour plots of girth welds ‘G’, ‘S1’ and ‘S2’. Dashed lines represent root-to-cap traverses.

The hardness distributions have been taken as an input for the definition of constitutive properties in a finite element model. To this end, element-specific material properties are assigned according to the hardness contour map of the investigated weld, based on the coordinates of each element’s centroid. This section further focuses on the assignment of material properties. Other aspects of the finite element model are described in more detail in section 2.2. It is emphasized that the equations below should not be considered as exact but merely serve as a tool to produce representative (i.e. realistic given the hardness value) potential stress-strain properties with variable yield strength and strain hardening behaviour, thus eliminating the fourth simplification of section 1.

The translation of hardness values into constitutive properties can be summarized in three steps. First, ultimate tensile strength R_m (MPa) is approximately related to macro Vickers hardness HV according to EN ISO 18265 (2003). Linear regression of tables in this standard leads to $R_m \approx 3.21 \cdot \mathrm{HV5}$. Second, yield-to-tensile ratio Y/T is delimited by an upper bound equation developed by Bannister et al. (2000) and included in FITNET (2008), using engineering 0.2% proof stress as an input. In a study focusing on weld metal (Hertelé et al., 2013a), Y/T was on average found to be 0.05 below the FITNET upper bound. This average relation could be expressed as a function of R_m by the following approximate relation:

$$Y/T \approx \frac{1}{1.07+(350/R_m)^{4.8}} \tag{3}$$

Further taking σ_y (Eq. 1) equal to the 0.2% proof stress (as also assumed to derive the equation above), it is easily obtained as $R_m \cdot Y/T$. This choice for σ_y implies that α is equal to $0.002/\varepsilon_y$ (with $\varepsilon_y = \sigma_y/E$ where E has been taken $200 \cdot 10^3$ MPa, a round number which is close to the actual value for steel).

Third, the strain hardening exponent n is theoretically closely related to Y/T, as follows from Considère's necking criterion for true stress and true strain ($d\sigma/d\varepsilon = \sigma$). An approximate solution is provided in R6 (2001) but its accuracy is questionable due to a number of analytical simplifications made (Hertelé et al., 2013a). For the purpose of this study, a more accurate solution has been curve fitted to provide a better agreement with Considère's criterion:

$$n = 2.4 + 2.9\frac{Y/T}{1-0.95\,Y/T} \tag{4}$$

The developed relations between the model parameters and Vickers hardness (HV5) are depicted in Fig. 3.

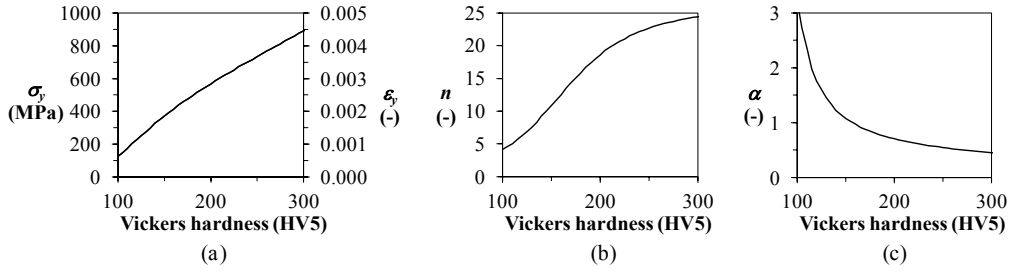

Fig. 3. Adopted transfer functions between Vickers hardness and Ramberg-Osgood model parameters: (a) σ_y and ε_y; (b) n; (c) α.

2.2. Finite element model

Three-dimensional side grooved $SE(T)_c$ specimens have been investigated using a parametric finite element model developed by Verstraete et al. (2014) with the software package ABAQUS® (version 6.11). The specimen geometry has been adopted from CANMET's $SE(T)_c$ testing procedure (Shen et al., 2009) and is characterized by a square cross section (thickness W = width B), a side-grooved notch ligament (total thickness reduction 15%), and a 'daylight grip length' L equal to $10W$ (Fig. 4). In agreement with $SE(T)_c$ testing practice, excessive weld root and cap material are removed. A blunt notch with initial radius 75 µm originates from the weld root surface. One half of the specimen is modelled assuming transverse symmetry. Roughly 18,000 eight-node linear brick elements with reduced integration have been used. A finite strain formulation has been adopted to allow for collapse phenomena under severe deformation. Isotropic J_2 plasticity (i.e., assuming the Von Mises yield criterion) has been imposed. Grayscale values in Fig. 4 are related to hardness and, following section 2.1, constitutive behaviour. Particular notch tip locations were aimed for. For instance, Fig. 4 depicts a notch placed in the weld metal centre (WMC).

2.3. Parametric study

Three variables have been examined in a parametric study: the weld ('G', 'S1' or 'S2'), the relative notch depth a/W (0.2, 0.3, 0.4, 0.5), and the notch tip location (WMC notch or HAZ notch). In total, 24 (= $3 \cdot 4 \cdot 2$) configurations have been investigated. Two simulations have been performed per configuration: one containing the actual weld, and one containing its equivalent idealised weld. As regards the latter, three particular challenges arise. First, the absence of symmetry with respect to the notch face implies that two different points '**F**' (Fig. 1) should be determined: one at either side of the notch ('$\mathbf{F_L}$' and '$\mathbf{F_R}$', respectively positioned at distances $H_{eq,L}$ and $H_{eq,R}$ from

the notched section), Fig. 5. In this study, it is chosen to define M_{eq} as an average of properties at both sides of the notch:

$$M_{eq} = \frac{\int_{\mathbf{F_L}\mathbf{OF_R}} M(s)\mathrm{d}s}{\|\mathbf{OF_L}\| + \|\mathbf{OF_R}\|} \tag{5}$$

where, given the nature of the known variables, $M(s)$ now refers to a mismatch of weld Vickers hardness relative to the average of the connected base metals: $M(s) = \mathrm{HV}_w(s)/\mathrm{HV}_b$.

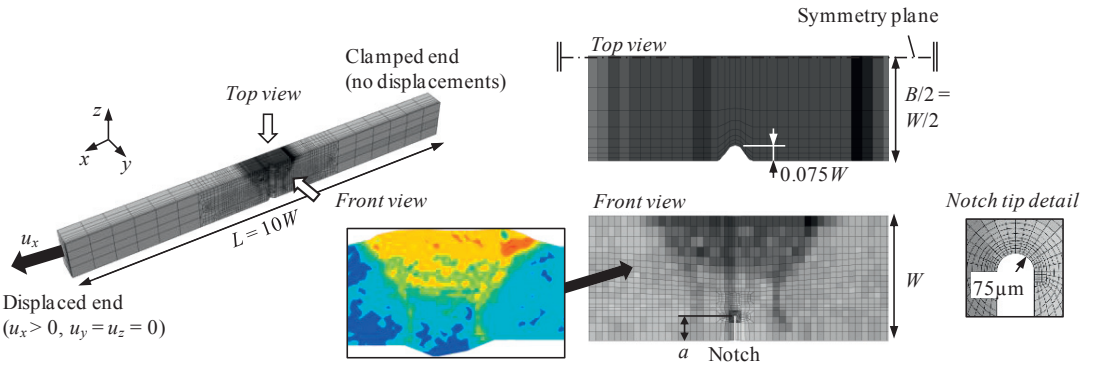

Fig. 4. Overview of the finite element model. Grayscale values represent element-specific hardness. Configuration shown: weld 'S1', $a/W = 0.2$, notch located in weld metal centre (WMC).

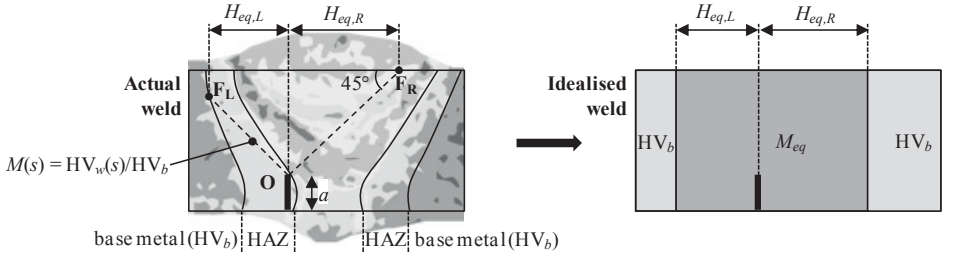

Fig. 5. Application of the weld idealisation approach for this study, illustrated for HAZ notched weld 'S2'.

Second, the presence of heat affected zones requires consideration as such zones are not present in an idealised weld. For this study, HAZ hardness has been incorporated in Eq. (5) by placing $\mathbf{F_L}$ and $\mathbf{F_R}$ at the base metal / HAZ interfaces rather than the fusion lines. Note that, in Fig. 5, $\mathbf{F_R}$ does not reach this interface as the right slip line is geometrically limited by the top surface of the specimen.

Third, the variation of strain hardening behaviour implies that an 'equivalent strain hardening exponent', n_{eq}, is to be determined for the weld metal of the idealised configuration. To this end, the procedure of section 2.1 is adopted, using the idealised weld metal hardness (HV_b;M_{eq}) as an input.

The validation consists of comparing simulation results of both configurations ('actual' and 'idealised') on the basis of their load bearing capacity on the one hand, and their crack driving force response on the other hand. Crack tip opening displacement (CTOD) has been preferred over J, given that the contour integral to obtain the latter is expected to be path dependent in heterogeneous welds. CTOD has been extracted at mid-width of the specimens (i.e. in the symmetry plane, Fig. 4), by tracking the displacements of crack face nodes 0.36 mm away from the crack tip

as earlier proposed by Fairchild et al. (2011). For a limited number of simulations, it was verified that this CTOD definition produces highly similar results to the 90° intercept method of Rice (1968), which is more challenging in terms of postprocessing.

3. Results and discussion

3.1. Slip line patterns

The assumed straight slip line patterns at either side of the notch are approximately confirmed by the analysis. However, there are small discrepancies between the assumed slip line angle (45°) and its actual value, as illustrated in Fig. 6. Slip line deviations can be theoretically attributed to material heterogeneity, as explained by Hao et al. (1997). Hence, errors may be introduced as a result of deriving M_{eq} from properties along 45° lines arising from the notch tip. These homogenisation errors are investigated in the following sections, subsequently focusing on load bearing capacity (section 3.2) and on crack driving force response (section 3.3).

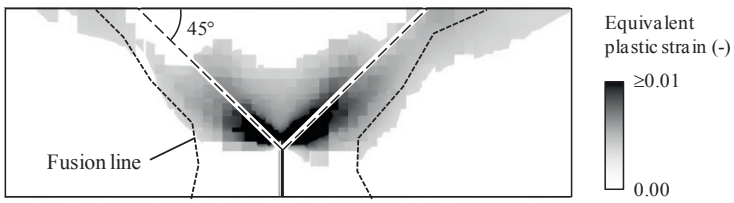

Fig. 6. The assumed slip line angle of 45° is not fully respected. Configuration shown: weld 'S1', WMC notch, $a/W = 0.3$.

3.2. Load bearing capacity

Figure 7 compares the load bearing capacities P_{max} (maximum load, indicating the onset of ligament collapse) of all specimens containing actual welds and their idealised equivalents. Each weld is depicted by a specific marker which is either solid (WMC notches) or open (HAZ notches). There are four data points for each marker type, corresponding to different relative notch depths (a/W = 0.2, 0.3, 0.4, 0.5). Hereby, deeper notches produce lower load bearing capacities. Dashed lines indicating a perfect one-to-one correspondence and errors of ±5% are drawn as a reference.

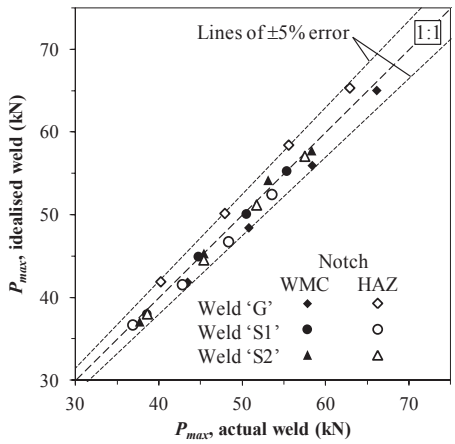

Fig. 7. Comparison of load bearing capacities of actual and idealised welds, indicating a strong correspondence.

The following observations are made from Fig. 7:

- None of the idealised welds show a load bearing capacity which is outside the ±5% error lines. This indicates that the removal of the simplifications listed in section 1 does not significantly affect the soundness of the homogenisation approach. Indeed, errors within the same order of magnitude were found for the initial validation study of Hertelé et al. (2013b), which incorporated all five simplifications of section 1.
- The magnitude of errors made is fair for both WMC and HAZ notched $SE(T)_c$ specimens. This observation implies that an absence of symmetry with respect to the notched section – particularly apparent for HAZ notches – does not alter the representativeness of an idealised weld.
- Idealised welds can either underestimate (e.g. weld 'G', WMC notch) or overestimate (e.g. weld 'G', HAZ notch) the load bearing capacity of an actual weld. Hence, simplifications of weld heterogeneity may alter the safety level of a flaw assessment in different directions (either adding or reducing conservatism).
- Of all three welds, 'S1' shows the smallest errors due to homogenisation. Remarkably, this is the weld with the greatest level of heterogeneity (a range of 36% in weld hardness mismatch, Table 1). Vice versa, the largest errors occur for weld 'G', which has the smallest level of heterogeneity (21% mismatch range). Since the opposite trend could be intuitively expected, the level of heterogeneity is hypothesized not to be a key parameter to the accuracy of crack driving force in an idealised weld. Other features such as notch location, HAZ properties and spatial distribution of weld heterogeneity may play a more significant role.

3.3. Crack driving force responses

The observations of section 3.2 can be extrapolated to the entire crack driving force responses (CTOD as a function of tensile load). As a case study, Fig. 8(a) focuses on weld 'G' containing HAZ notches of varying depth – the configuration which produces the largest errors for load bearing capacity in Fig. 7 (4.6% on average). For each notch depth, the error on P_{max} appears to be representative of nearly the entire crack driving force response (notwithstanding the linear elastic stage, where the difference between actual and idealised welds vanishes). This statement is confirmed in Fig. 8(b), which depicts crack driving forces of the configuration with the best agreement between actual and idealised welds (weld 'S1', WMC notch, on average 0.2% error on P_{max}) as a second example.

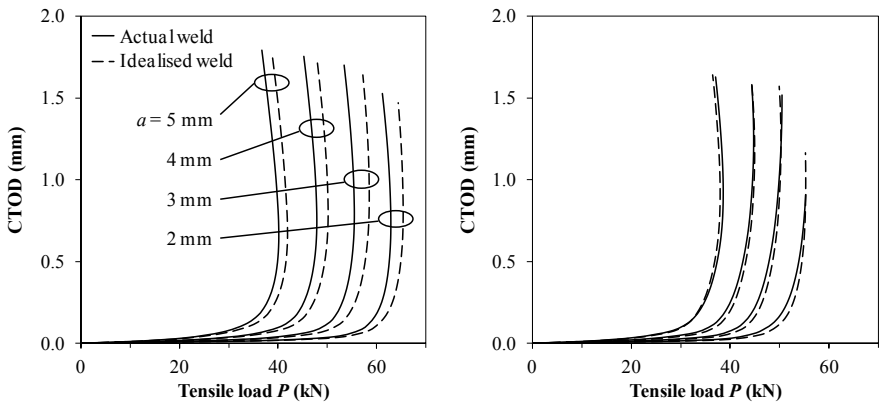

(a) Weld 'G', HAZ notch (b) Weld 'S1', WMC notch

Fig. 8. Crack driving force responses of two selected configurations. The legend for subfigure (b) is adopted from subfigure (a).

4. Conclusions

An explicit procedure to simplify complex heterogeneous welds into idealised welds allows for accurate estimations of collapse load and of crack driving force response. Whereas earlier work focused on theoretical (i.e., two-dimensional, symmetrical) welds without heat affected zones, the current study extends the applicability of the method to more realistic cases. Concretely, the error due to weld idealisation remains within fair limits (±5% in terms of load) for three-dimensional clamped SE(T) specimens with asymmetrical material distributions (e.g. HAZ notched welds) involving severe weld heterogeneity in terms of both yield strength and strain hardening behaviour, and variable HAZ properties. Weld idealisation may either increase or decrease the safety level of a flaw assessment. When applied, it is advised to introduce a partial safety factor that accounts for this unpredictability. For the investigated welds, it would be safe to reduce loads predicted from idealised welds (given a certain crack driving force) by 5%.

Acknowledgements

The authors would like to acknowledge the financial support of the BOF (Special Research Fund – Ghent University, postdoctoral grant nr. BOF12/PDO/049) and the FWO Vlaanderen (Research Foundation – Flanders, international mobility grant nr. V418113N).

References

Bannister, A.C., Ocejo, J.R., Gutierrez-Solana, F., 2000. Implications of the Yield/Tensile Stress Ratio to the SINTAP Failure Assessment Diagrams for Homogeneous Materials. Engineering Fracture Mechanics 67(6), 547–562.

EN ISO 18265, 2003. Metallic materials – Conversion of hardness values. International Organisation for Standardization, Switzerland.

Fairchild, D.P., Macia, M.L., Kibey, S., Wang, X., Krishnan, V.R., Bardi, F., Tang, H., Cheng, W., 2011. A multi-tiered procedure for engineering critical assessment of strain-based pipelines. 21st International Offshore and Polar Engineering Conference, Maui, Hawaii, USA, 698–705.

FITNET, 2008. Fitness for service procedure, MK8, Vol. 1: Procedure. GKSS Research Centre, Geesthacht, Germany.

Hertelé, S., Gubeljak, N., De Waele, W., 2013a. Advanced characterization of heterogeneous arc welds using micro tensile tests and UGent stress-strain model. Submitted.

Hertelé, S., De Waele, W., Verstraete, M., Denys, R., O'Dowd, N.P., 2013b. *J*-integral analysis of heterogeneous flawed girth welds in clamped single-edge notched tension specimens. Submitted.

Hao, S., Cornec, A., Schwalbe, K.H., 1997. Plastic stress-strain fields and limit loads of a plane strain cracked tensile panel with a mismatched welded joint. International Journal of Solids and Structures 34(3), 297–326.

Kim, Y.J., 2002. Estimation of Fully Plastic Crack Tip Stresses from Equilibrium of Least Upper Bound Circular Arcs. International Journal of Mechanical Sciences 44(5), 881–897.

Kim, Y.J., Schwalbe, K.H., 2001. Compendium of Yield Load Solutions for Strength Mis-Matched DE(T), SE(B) and C(T) specimens. Engineering Fracture Mechanics 68(9), 1131–1151.

Kumar, V., German, M.D., Shih, C.F., 1981. An engineering approach for elastic-plastic fracture analysis. EPRI-Report-NP-1931, EPRI.

R6, 2001. Assessment of the integrity of structures containing defects. Revision 4. EDF Energy Nuclear Generation Ltd, UK.

Ramberg, W., Osgood, W.R., 1943. Description of stress-strain curves by three parameters. Technical note No. 902, National Advisory Committee for Aeronautics.

Rice, J.R., 1968. A Path Independent Integral and the Approximate Analysis of Strain Concentration by Notches and Cracks. Journal of Applied Mechanics 35, 379–386.

Schwalbe, K.H., Koçak, M., editors, 1994. Proceedings of the International Conference on Mis-Matching of Welds. ESIS 17, Mechanical Engineering Publications Ltd, London, UK.

Schwalbe, K.H., Koçak, M., editors, 1997. Proceedings of the Second International Symposium on Mis-Matching of Interfaces and Welds. GKSS Research Centre, Geesthacht, Germany.

Shen, G., Gianetto, J.A., Tyson, W.R., 2009. Measurement of *J-R* curves using single specimen technique on clamped SE(T) specimens. 19th International Offshore and Polar Engineering Conference, Osaka, Japan, 92–99.

Verstraete, M., Hertelé, S., Denys, R., Van Minnebruggen, K., De Waele, W., 2014. Evaluation and interpretation of ductile crack extension in SENT specimens using unloading compliance technique. Engineering Fracture Mechanics 115, 190–203.